

Displacement stability revisited – A new criterion for the onset of viscous fingering

Jos G. Maas^{1,*}, Niels Springer², Albert Hebing¹, and Steffen Berg³

¹PanTerra Geoconsultants BV, Leiderdorp, The Netherlands

²GEUS, København, Denmark

³Shell Global Solutions International B.V., Amsterdam, The Netherlands

Abstract. Any process in which a high mobility fluid is displacing a lower mobility fluid is prone to instability. Pertinent present-day examples are CO₂ injection for carbon capture and sequestration (CCS), gas injection for underground storage or for pressure maintenance. Over the years, several criteria have been developed to predict the onset of viscous fingering. However, there is no consensus on what criterion is truly valid and more recently several studies have been reported to empirically decide on what criterion is the most reliable. In this work, we present a new approach derived from first principles. The results are shown to unify all earlier derived criteria whether for porous rock, or for Hele-Shaw cells, with and without gravity, immiscible and miscible, through proving that these are special cases, of limited validity, of a more general formulation. The new criterion is more restrictive in terms of viscosity ratio than the Hagoort shock-front mobility ratio, but less restrictive than the straightforward viscosity ratio. 2-Phase flow simulations have been conducted to demonstrate the validity over a wide parameter range. In addition, we have studied the impact of fingering in SCAL laboratory tests employing the unsteady-state (“Welge”) technique. The results were analysed through interpretation-by-simulation using the automatic history matching tool AutoSCORES.

1 Introduction

The study of displacement stability has a very long history and goes back to at least 1857 when Jevons [1] reported on the cirrus form of cloud. Lord Rayleigh [2] was prompted by the observations of Jevons to analyse displacement stability using linear perturbation theory and presented a criterion for the onset of instability based on density gradients in 1883. It appears that the first sequel to this work only came about in the late 1940’s. de Korver and Douwes Dekker [3] (1949) derived a criterion for stable displacement of viscous oil by brine for the Schoonebeek field in the Netherlands. Their analysis is based on the behaviour of a macroscopic “gravity tongue” rather than on the analysis of the fate of a small wave-like perturbation that Lord Rayleigh conducted. As we will demonstrate in section 2, both approaches produce the same result. The criterion derived by de Korver and Douwes Dekker includes a critical displacement velocity that depends on both density and viscosity differences between the brine and the oil.

Also in 1949, Taylor [4] presented a linear perturbation analysis of wave-like perturbations of an accelerating interface between two immiscible liquids moving in open space, i.e. not within a porous medium, so viscosities do not enter. He showed that perturbations will grow initially exponentially or rather shrink exponentially dependent on the density difference. In a companion paper, Lewis [5] presented experimental results on finger growth in a

“vertical channel” that were in line with the theoretical predictions.

Hill [6] (1952) published the derivation for the onset of instability in a sugar solution displaced by water in a vertical column filled with charcoal, as used in industrial sugar refining operations. Through an analysis of pressure gradients at both sides of the interface between the two liquids, he showed that both density and viscosity differences control a critical displacement velocity for instabilities to develop. He tested the theory successfully with experiments conducted in rectangular perspex cells, filled with glass beads.

Dietz’s [7] (1953) well-known (see e.g. [8, 9]) stability criterion is a direct extension of the work published by de Kramer and Douwes Dekker [3].

Saffman and Taylor [10] published their land-mark paper in 1958. They introduced the effect of interfacial tension (IFT) as counter-acting mechanism against the viscous-unstable growth into the linear perturbation analysis and show that a continuum of wavelengths λ would exist for fingers to develop, with the stability index (initial exponential growth factor) dependent on λ . A critical wavelength and a critical displacement velocity were identified. On a general note, they claim the experimental conditions in so-called Hele-Shaw [11] cells (two parallel glass plates with an open channel in between) to be representative for the study of displacement stability in porous media. It is of interest that Saffman and Taylor make

* Corresponding author: jgmaas@gmail.com

a remark on Dietz's work: "did not explicitly consider stability of the interface". In section 2, as for the case with the analysis by Lord Rayleigh, we will demonstrate that as far as determining the onset of instability, both approaches give the same result. Another point of interest is that the introduction of IFT created an important problem: the solution for the stability index becomes unbound for IFT moving to zero. This problem has been studied by a number of authors [e.g. 12, 13, and 14]

As also observed by Homsy [15] in his overview paper, Chuoke¹ et al. [16] (1959) published an approach into developing a stability criterion closely related to the work by Saffman and Taylor [10] (who actually referenced Chuoke). Chuoke et al. show that a wavelength of maximum instability growth rate can be identified (by subsequent authors referred to as "most dangerous" wavelength or wave number, see e.g. [17, 18, and 19]). Note that Chuoke et al. [16] use a loosely defined "effective" IFT that needs to be determined experimentally and may depend on rock and fluids (and on IFT between the two fluids for that matter).

Dumoré [20], building on Hill's work [6], derived a stability criterion in 1964 including a critical displacement velocity for a miscible drive under reservoir conditions.

In 1974 Hagoort [21] derived a new stability criterion by assuming that saturations upstream of the displacement front in porous rock are close to the shock front saturation. Hagoort derived his criterion first with the assumption that the capillary pressure between brine and oil equals zero. He then proposed an "energetic" approach to include the effect of capillary pressure.

Finally, the work by Chuoke et al. [16] was extended by Peters and Flock [22] (1979) with the introduction of spatial boundary conditions for displacements with circular and rectangular cross-sections. Due to these boundary conditions, the continuum spectrum of wavelengths of the perturbations was replaced by a discrete spectrum. As a result, two new stability criteria (one for the circular and one for the rectangular case) appeared that honour the exclusion of the continuum spectrum of wavelengths.

To the best of our knowledge, Peters and Flock are the last authors who proposed a criterion for the onset of instability that can be calculated analytically.

Numerous authors [see e.g. 23, 24, 25, 26, 27, and 28] have studied the growth of fingers once that these become into existence. Often, a criterion for the onset of instability is not mentioned explicitly. If it is, various choices seem to have been made: just the viscosity ratio M_μ (see nomenclature at the end of this paper) being larger than unity, or the end-point mobility ratio M_{end} larger than unity, without prove of validity.

Others have conducted experiments and/or simulations [29] to establish which criterion is closest to reality. The experiments fall into three classes: a) experiments in Hele-Shaw cells or micro models, using optical means to detect or monitor fingering [e.g. 30, 31, and 32]; b) experiments on porous media using X-ray CT [e.g. 33, 34]; c) experiments that infer instability from the value of a chosen criterion [e.g. 35, 36].

Some 10 years ago, Tang and Kovscek [37] showed experimental results demonstrating an example of unstable displacement with $M_{s_hag} < 1$, putting the approach of Hagoort [21] in doubt. Ott et al. [38] defined instabilities observed for $M_{s_hag} < 1$ as "channelling" features as opposed to fingering observed for $M_{s_hag} > 1$. More recently, the uncertainty around the validity of M_{s_hag} as a stability criterion was further demonstrated by Bouquet et al. [39], who investigated four different mobility criteria, testing these against numerical results. The results favoured Hagoort's M_{s_hag} criterion. However, the overall impression remained that the M_{s_hag} criterion for stability is basically an empirical criterion that like the other criteria works best for specific situations. Today, still no consensus exists as to what the correct criterion is to predict the onset of fingering in the general case.

With increasing interest in injection processes (as opposed to simple depletion) and increased focus on gas-injection such as CO₂ and H₂, a solid criterion that predicts the onset of unstable displacement will prove its value in the design of carbon sequestration projects, underground gas storage, but also for water drives, polymer or other chemical injection projects, low salinity flooding and CO₂ EOR projects.

1.1 Considerations developing a stability criterion

To predict fingering, it is not sufficient to focus only on the stability of the shock front. The classical Saffman-Taylor criterion is strictly speaking only valid for very small finger amplitudes and does not cover the growth of large amplitudes. Therefore, the question whether perturbations of a shock front can really grow further involves – because of the displacement-related fractional flow physics – a wider range of saturations (and relative permeability and capillary pressure) outside the shock front. The other extreme is the endpoint mobility ratio criterion that basically says that in the end fingers can only grow if they are unstable over the full mobile saturation range. That is too restrictive, because an actual displacement may not cover the saturation range all the way to the endpoints. In Hele-Shaw cells this issue does not occur, because there, due to the simple geometry, relative permeability and capillary pressure are constant and independent of saturation.

In this paper, we present a holistic criterion to predict the onset of instability of a drive against fingering. The new criterion is built up from first principles and is based on a new concept that generalises the conditions necessary for unstable displacement. In essence, we start out by following Hill [6], who realised that for a perturbation to grow, the pressure gradients near the interface needs to promote that. Hill then assumed constant saturations and effective permeabilities to analyse the pressure profile upstream and downstream of the interface. In contrast, our approach recognises the fact that a so-called Buckley-Leverett [8, 40] profile will appear, due to fractional flow physics, which impacts the pressure gradients around the displacement front. Additional considerations are explained in the next section.

The new criterion still has the form of a test on mobility ratio. It differs from the existing tests in that it accounts not

¹ Mistakenly spelled by Homsy as Chouke

only for viscosities and relative permeability values at some chosen saturation, but rather depends on viscosities and on the shape of the relative permeability curves. The new criterion is found generally to be less restrictive than the end-point mobility criterion but more restrictive than Hagoort's M_{s_hag} [21].

We present in the next section the derivation of the new criterion and show how the earlier derived criteria are special cases of a more general formulation. In section 3, we discuss simulation results studying the new criterion and demonstrate why the results in the literature can appear contradictory. Section 4 deals with the possible impact of fingering on SCAL measurement results. Section 5 discusses the experimental work that has been carried out. Conclusions are presented in section 6.

2 The onset of unstable displacement

To be clear, we define “onset” here as the mathematical condition *necessary* for a small frontal perturbation not to die out immediately after that it comes about, irrespective of how the perturbation occurred. We emphasize that this mathematical condition may well be *not sufficient*: other parameters may still impede a perturbation to grow. An example of that is capillary pressure, which will be addressed in section 2.8.

With this definition in mind, consider an unsteady-state (“Welge”) experiment at constant injection rate of a fluid 1, displacing a fluid 2, with a displacement front moving through a homogeneous porous medium in the x-direction. Injection of fluid 1 occurs over the whole y-z plane at $x=0$, production exits the porous medium through the y-z plane at $x=L$, far away. The displacement front is flat and extends in the y- and z-direction. The porous rock is initially saturated with fluid 2 (only). Fractional-flow physics [40] prescribes the build-up of a shock front.

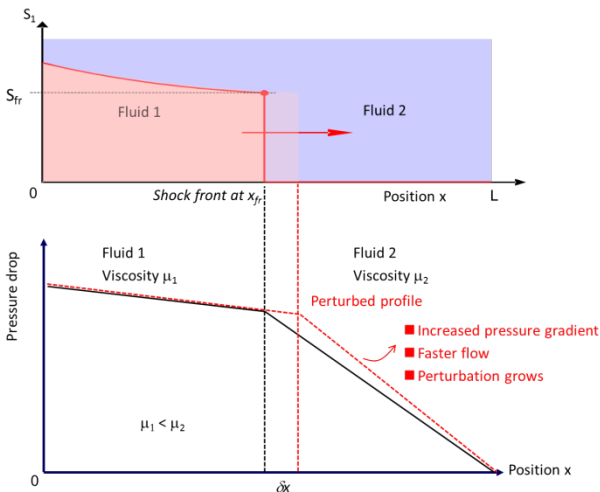


Fig. 1. Saturation and pressure profile through an unperturbed stream tube, combined with the profiles in the stream tube with a single, sudden and infinitesimally small perturbation.

Fig. 1 shows a typical saturation profile and pressure profile through a stream tube along the x-direction at some time t . Let's further assume that at this time t , a sudden and infinitesimally small perturbation appears only at one point

(y_p, z_p) in the otherwise flat y-z front and reaches into position $x_{fr} + \delta x$.

The early fate of the perturbation, i.e. whether it can grow and outrun the flat front, or rather be taken over by the flat front is the anchoring point for our stability analysis. To study the early fate of this perturbation over time one needs to solve the flow equations. As a first step, following the reasoning of Lord Rayleigh [2], Taylor [4] and many others [e.g. 22, 26, and 41] we can approximate the pressure function and saturation distribution far upstream and downstream of the front by the unperturbed values. This is equivalent to solving the flow equations of the perturbed system under the boundary condition of a constant pressure drop ΔP across the sample. The unperturbed pressure drop follows from the parameters controlling the unsteady-state experiment just before the perturbation occurred.

The second step we took is to use the fact that according to fractional flow theory each saturation travels at its own speed [40]. When we consider the perturbation in Fig. 1 from that perspective, we note that the position of the front at the perturbation deviates from the flat front, but the shock front saturation itself is unchanged. For the shock front saturation we have² according to [40]:

$$v_{fr} = \frac{q}{\phi} \left(\frac{\partial f_w}{\partial s} \right)_{s_{fr}} \quad (1)$$

From inspection of the flow equations it follows that we can interpret the perturbation as this part of the front been shifted in time by an infinitesimally small amount. Therefore, the early fate of the perturbation is determined by how the velocity of the front at the perturbation, or equivalently (see Eq. 1) the flow rate q through a stream tube through the perturbation would change at an infinitesimally-small time shift, with the pressure drop across the stream tube kept constant. In line with our definition of “onset”, see above, the necessary condition for a perturbation not to die immediately translates into the requirement that the velocity of the interface should increase with t at constant ΔP . Using (1), the new concept to determine the onset of instability therefore is expressed mathematically by the condition

$$\left(\frac{\partial q}{\partial t} \right)_{\Delta P} > 0 \quad (2)$$

This concept reduces the dimensions of the frontal perturbation of a 2D or 3D interface/displacement front to effectively one dimension, studying acceleration of flow in a stream tube at constant ΔP .

It is important to note that our concept makes use of the same equations and same assumptions implicitly used by previous authors. The criterion comes about naturally when the assumptions are made explicit, in particular the notion that equations are solved under the boundary condition of a constant ΔP . The important difference between this approach and the work by previous authors is that these all chose to approximate saturations upstream and downstream of the interface to be at some constant value, while we apply

² For an explanation of symbols, see the Nomenclature at the end of the paper.

fractional flow theory that predicts a Buckley-Leverett profile. The constant saturations certainly are a good approximation in Hele-Shaw cells, but much less so in porous media.

Starting with condition 2 we can derive a relation to use in the laboratory or the field in practical terms to predict the onset of instability. From Darcy's equation (neglecting gravity for the moment) we have for 2-phase flow

$$q_{tot} = -K \left[\frac{k_{rw}(S)}{\mu_w} + \frac{k_{ro}(S)}{\mu_o} \right] \frac{dp}{dx} \quad (3)$$

In order to simplify the notation, define

$$R = R(x, t) = \left[\frac{k_{rw}(S)}{\mu_w} + \frac{k_{ro}(S)}{\mu_o} \right]^{-1} \quad (4)$$

and

$$G = G(t) = \int_0^{x_{fr}} R dx + \int_{x_{fr}}^L R dx \quad (5)$$

We get

$$\Delta P = K^{-1} q G \quad (6)$$

So

$$\left(\frac{dq}{dt} \right)_{\Delta P} = \frac{-q}{G} \frac{dG}{dt} \quad (7)$$

Combining Eq. 7 with condition 2, we find that unstable displacement will occur for

$$\frac{dG}{dt} < 0 \quad (8)$$

Condition 8 allows us to work out a number of examples for comparison with historic criteria for stability.

2.1 Onset of instability in Hele-Shaw cells

The conditions in Hele-Shaw cells are $S_{upstream}=1$ and $S_{downstream} = 0$, with S the saturation of the injected phase. When injecting water to displace oil, we find for G (see Eqs. 5 and 4)

$$G = x_{fr} \mu_w + (L - x_{fr}) \mu_o \quad (9)$$

Therefore

$$\frac{dG}{dt} = \frac{dx_{fr}}{dt} (\mu_w - \mu_o) \quad (10)$$

Combining Eq. 10 with condition 8, we find that the displacement will be unstable for $\mu_o > \mu_w$, as expected.

2.2 Onset of instability in the cases of Saffman and Taylor and Chuoke

Both Saffman and Taylor [4] and Chuoke [16] assume that the upstream saturation is constant and equal to $1-S_{or}$, while the downstream saturation equals S_{wc} when water is displacing oil. Similar to the derivation for the Hele-Shaw cells, we now find

$$\frac{dG}{dt} = \frac{dx_{fr}}{dt} \left\{ \left[\frac{k_{rwor}}{\mu_w} \right]^{-1} - \left[\frac{k_{rowc}}{\mu_o} \right]^{-1} \right\} \quad (11)$$

Combining Eq. 11 with condition 8, we find that the displacement will be unstable for

$$\frac{k_{rwor}}{\mu_w} > \frac{k_{rowc}}{\mu_o} \quad (12)$$

i.e. for $M_{end} > 1$, identical to the results obtained by these authors.

2.3 Onset of instability according to Hagoort

Hagoort [21] argued that the upstream saturation could be approximated by the shock front saturation. Similar to the cases treated above, we find now

$$\frac{dG}{dt} = \frac{dx_{fr}}{dt} \left\{ \left[\frac{k_{rw}(S_{fr})}{\mu_w} + \frac{k_{ro}(S_{fr})}{\mu_o} \right]^{-1} - \left[\frac{k_{rowc}}{\mu_o} \right]^{-1} \right\} \quad (13)$$

Combining Eq. 13 with condition 8 results immediately into the criterion as derived by Hagoort: the drive is unstable for

$$\frac{k_{rw}(S_{fr})}{\mu_w} + \frac{k_{ro}(S_{fr})}{\mu_o} > \frac{k_{rowc}}{\mu_o} \quad (14)$$

2.4 Onset of instability in Steady-State experiments

Lenormand et al. [42] show in their Fig. 4 a pressure drop profile as it typically occurs in steady-state experiments: the pressure drop first increases at each step in fractional flow and then decreases. From the examples discussed above, it becomes clear that the criterion of instability as presented in condition 8 will play its role in Steady-State experiments. We consider here two consecutive steps: a step with fractional flow f_1 followed by a step at f_2 . We define $S_{upstream} = S_2(f_2)$ and $S_{downstream} = S_1(f_1)$. Similar again to previous cases, we find

$$\frac{dG}{dt} = \frac{dx_{fr}}{dt} \left\{ \left[\frac{k_{rw}(S_2)}{\mu_w} + \frac{k_{ro}(S_2)}{\mu_o} \right]^{-1} - \left[\frac{k_{rw}(S_1)}{\mu_w} + \frac{k_{ro}(S_1)}{\mu_o} \right]^{-1} \right\} \quad (15)$$

Combining Eq. 15 with condition 8 predicts the displacement to be unstable for

$$\frac{k_{rw}(S_2)}{\mu_w} + \frac{k_{ro}(S_2)}{\mu_o} > \frac{k_{rw}(S_1)}{\mu_w} + \frac{k_{ro}(S_1)}{\mu_o} \quad (16)$$

Berg et al. [43] show in their Fig. 3 that oscillations become apparent at or near the top of the differential pressure plot vs time. The criterion in condition 16 may well be the trigger for the oscillations. Note that our present results are limited to understanding the onset for instability and cannot be used to analyse the oscillations themselves.

2.5 Onset of instability with impact of gravity for miscible displacement according to Dumoré

Dumoré [20] studied the onset for instability in a vertically downward displacement of oil by solvent injection, under the assumptions of constant saturations upstream and downstream of the displacement front. Notably, he assumed $k_{rw}=k_{rowc}=1$, with no oil flowing upstream and no solvent flowing downstream. Moreover, he assumed constant viscosities upstream and downstream. Inserting this data

into condition A9 (see Appendix), it follows immediately that the displacement is stable for

$$q < gK \frac{(\rho_o - \rho_s)}{(\mu_o - \mu_s)} \quad (17)$$

This is identical to the result obtained by Dumoré, who identified the right-hand side of condition 17 as a critical displacement rate for stable miscible, vertical, displacement.

2.6 Onset of instability with impact of gravity for immiscible displacement according to Dietz

Dietz [7] (or in fact de Korver and Douwes Dekker [3]) studied the onset of instability of water-oil displacement in a reservoir dipping at an angle θ with respect to the horizontal. Similar to Dumoré [20], he assumed the saturations upstream and downstream to be constant. However, he used for the relative permeabilities the values at the saturation end-points k_{rwo} and k_{rowc} respectively. As in section 2.5, inserting this data into condition A9, calculation of the onset of instability is straightforward. We find the displacement to be stable for

$$1 - M_{end} > -\frac{K}{q} g \sin\theta \Delta\rho \frac{k_{rwo}}{\mu_w} \quad (18)$$

We have three cases:

a) $M_{end} = 1$

The displacement will be stable for $\Delta\rho > 0$ and unstable for $\Delta\rho < 0$

b) $M_{end} < 1$

The displacement will be stable for

$$q > -\frac{K}{(1 - M_{end})} g \sin\theta \Delta\rho \frac{k_{rwo}}{\mu_w} \quad (19)$$

c) $M_{end} > 1$

The displacement will be stable for

$$q < \frac{K}{(M_{end} - 1)} g \sin\theta \Delta\rho \frac{k_{rwo}}{\mu_w} \quad (20)$$

The results for cases a, b, and c are identical to what is shown in Dake [8] as a summary for ‘‘Dietz’’ tonguing.

It is noteworthy that our concept that considers infinitesimally small perturbations, leads to results identical as was found by Dietz or de Korver and Douwes Dekker, while these authors studied the stability of displacement at a macroscopic scale in the field.

2.7 Onset of instability in a more general case

For the case of water displacing oil, we find (for details see Appendix A) as a necessary condition for stable displacement in the absence of gravity two cases: a) $M_{end} \leq \alpha$: stable displacement, independent of the value of M_{s_hag} ; b) $M_{end} > \alpha$: stable displacement only if

$$M_{s_hag} < M_\alpha < 1 \quad (21)$$

with

$$M_\alpha = \frac{1 - \alpha}{1 - \frac{\alpha}{M_{end}}} \quad (22)$$

α given in Eq. A16, $0 < \alpha < 1$. So we have $0 < M_\alpha < 1$.

From the condition 21, we find that our new criterion is more restrictive than Hagoort’s [21] criterion, when seen as a function of the viscosity ratio: the original Hagoort criterion requires M_{s_hag} only to be less than unity, while now it needs to be less than M_α .

Note that the expression for α (Eq. A16) is amenable to numerical integration. As a result, for given viscosity ratio and fractional flow function, one can easily test for stability of the displacement. In our experience, α is in the order of 0.3 to 0.7, which allows for a quick check.

2.7.1 Impact of gravity

In Appendix A, we show the complete formulation accounting for the impact of gravity, injecting fluid 1 to displace fluid 2. Three situations come about: a) $M_{end} \leq \alpha$: stable displacement, independent of the value of M_{s_hag} and of flow rate; b) $M_{end} > \alpha$, $M_{s_hag} \leq M_\alpha$: stable displacement independent of the rate; c) $M_{end} > \alpha$, $M_{s_hag} > M_\alpha$: stable displacement only if the flow rate is less than a critical rate q_{crit} :

$$q_{crit} = \left\{ K \Delta\rho g \sin(\theta) \left[\frac{k_{r2_end}}{\mu_2} \right] \frac{1}{(1 - \alpha)} \frac{(M_{sh} + \beta)}{(M_{sh} + 1)} \left[\frac{1}{M_\alpha} - \frac{1}{M_{s_hag}} \right]^{-1} \right\} \quad (23)$$

with β given in Eq. A26, $0 < \beta < 1$ and M_{sh} defined in Eq. A29. It is of interest to note that the first term, between the accolades, equals Hagoort’s ‘‘free fall filter velocity’’ [44]. So, the remainder of condition 23 can be seen as an adjustment to the free fall velocity. Note also that the new critical rate is not dependent on (k_{r1_end}/μ_1) as is the case in the original Dietz criterion, see condition 20.

In summary, we see that gravity brings about a stabilising effect, up to a critical rate. This is in line with the classical stability criteria for viscous fingering derived by linear stability analysis [3, 7, and 20].

Although the formulas get much more complicated when accounting for gravity, these (including Eq. A26 for β) are still easily tractable by numerical integration and therefore allow for a screening of parameters for stable displacement.

2.8 Impact of capillary pressure on the onset of instability

The concept discussed above does allow for accounting for capillary pressure, but implementing capillary pressure into the flow equations would not result in a transparent criterion for the onset of instability. Too many parameters would appear. Instead, we have chosen to assess generically the impact of capillary pressure on the criterion as derived above. In addition, we have tested our assessment with simulations discussed in section 3.

2.8.1 Generic impact of capillary pressure on the onset of instability

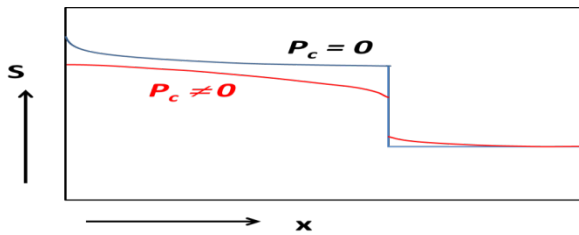


Fig. 2. Typical Buckley-Leverett saturation profile with zero capillary pressure (blue) and saturation profile accounting for capillary pressure (red).

Fig. 2 shows the impact of capillary pressure on the saturation distribution of a water-oil displacement. Upstream of the shock front, the water saturation is reduced with respect to Buckley-Leverett profile observed in the absence of capillary pressure. This is due to the positive branch of the imbibition capillary pressure. On the other hand, downstream, the water saturation is increased, due to the negative branch of the capillary pressure. As a result, the mobility contrast between upstream and downstream moving fluids is reduced with respect to the situation with a zero capillary pressure.

Our criterion for the onset of instability is reflecting that contrast, so we conclude that the onset of instability in the presence of capillary pressure will be shifted to higher values for the viscosity ratio.

For oil-water or gas-water drainage, the capillary pressure has only a positive branch. Therefore, the impact of capillary pressure will only be upstream of the displacement front. Still, the contrast in mobility upstream and downstream will be reduced, be it less. This is demonstrated in section 3.

3 The onset of fingering tested with simulations

As discussed in section 2, the criterion for the onset of instability in displacement processes is determined by the condition $(\partial q/\partial t)_{\Delta P} > 0$. The criterion analyses the early fate of an infinitesimal perturbation over an infinitesimally small time span. The analysis is independent of the actual boundary conditions, whether the injection rate is constant or whether the pressure drop is maintained constant.

We can now take this one step further: for a displacement at constant pressure drop, the condition $(\partial q/\partial t)_{\Delta P} > 0$ will bring about an accelerating flow rate throughout. This means the integrated total mobility is increasing. Therefore, for a displacement at constant injection rate, rather than at constant pressure drop, with the same input parameters for viscosity, relative permeability, etc., when the onset of instability is met, the pressure drop will have to decline, in line with the increasing integrated total mobility. This can easily be proven mathematically by inspecting $(\partial \Delta P/\partial t)_q$. Moreover, we have verified this “rule” with simulations, as discussed below.

3.1 One-dimensional simulations

First we have run a number of unsteady-state simulations with SCORES [42, 45] in 1-D. We ran simulations in drainage mode, incompressible flow, with a viscosity for the injected phase of 0.02cP to mimic CO₂ injection. Corey parameters, porosity and permeability were set to the same values as used in our earlier work on OBKN outcrop [46], that also shows what definition was used for Corey parameters.

To fully screen the displacement behaviour for stability, we ran 10 different cases, varying the viscosity of the displaced phase from 0.01cP (which corresponded to $M_\mu = 0.5$, $M_{\text{end}} = 0.28$, $M_{s_hag} = 0.11$, $M_\alpha = 17.5$, so judged by all criteria as stable) to 10cP (which corresponded to $M_\mu = 500$, $M_{\text{end}} = 281$, $M_{s_hag} = 1.84$, $M_\alpha = 0.59$, so unstable by all criteria).

With P_c set to zero, we found perfect correspondence between the behaviour of the pressure drop and the integrated total mobility concept: $\Delta P(t)$ was increasing before breakthrough when our new criterion would predict a stable displacement and it remained constant exactly at the calculated point of onset. The pressure drop was declining before breakthrough for cases where the point of onset was surpassed. There was no dependence on flow rate, as expected.

We then applied the capillary pressure curve used in earlier work by Maas et al. [46]. The behaviour of $\Delta P(t)$ changed in line with expectations. At low flow rate, the tipping point for an increasing $\Delta P(t)$ before breakthrough into a decreasing of $\Delta P(t)$ moved to a higher viscosity ratio. At high flow rate, the tipping point did not move noticeably compared to the zero P_c cases. This is due to the viscous forces being strong enough to reduce the effect of P_c .

3.2 Simulations in 2-D

Of course, in one-dimensional simulations one can only observe the character of $\Delta P(t)$, but fingering itself cannot occur. Therefore, we moved subsequently to simulations in 2-D. It is well known that fingering in simulations can only be observed if the right triggering [e.g. 47, 48, and 49] is incorporated. We used a Gaussian distribution for porosity, with a standard deviation of 0.02. Permeability in each individual grid block was then set through an exponential correlation, as used by Maas et al. [46]. Therefore, the permeability distribution is log-normal. The permeability variation factor V [50] (similar to the Dykstra Parsons [51] coefficient) equalled 0.42, which is still quite homogeneous in view of the V cut-off of 0.9 [46] and therefore acceptable for SCAL experiments. Gridding was as used by Berg and Ott [29]: 400 (perpendicular to flow) x 200 grid blocks in the flow direction. The behaviour of $\Delta P(t)$ before breakthrough was very similar to the 1-D cases discussed above, both for P_c set to zero and for P_c set as in Maas et al. [46]. Note that P_c was different for each individual grid block: we used one dimensionless Leverett-J function, scaled per grid block with the square root of the individual porosity divided by the individual permeability.

3.2.1 Fingering observed in the saturation maps

Fingering is clearly visible in the saturation map at high viscosity ratio, both with P_c set to zero and with the P_c inputted as mentioned above, with only a nominal difference in appearance. At the lowest viscosity ratio where all criteria predict stable displacement, the difference was more visible. At zero P_c , the saturation map showed a well-defined sharp and flat front, while the rock is definitely heterogeneous with its Gaussian porosity and log-normal permeability distribution. However, with the P_c switched on, and at low flow rate, the front became slightly irregular at the lowest viscosity ratio, see Fig. 3. In addition, these irregularities did not grow with the advancing front. At high flow rate, the irregularities disappeared. Apparently, high viscous forces reduce the impact of a non-zero capillary pressure, similar as discussed above.

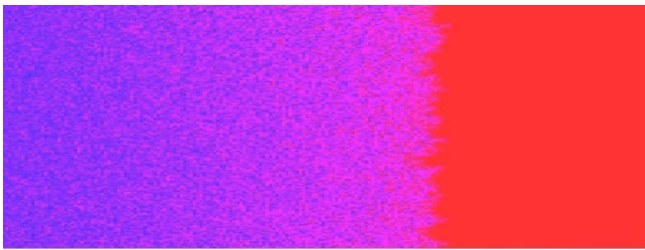


Fig. 3. Displacement front for CO₂ injection at extreme favourable viscosity ratio ($\mu_{CO_2} = 0.02\text{cP}$, $\mu_w = 0.01\text{cP}$). The frontal irregularities do not grow over time: “capillary fingering”.

Note that these simulations are in primary drainage mode, so the capillary pressure function has no negative branch and therefore no injected fluid will be “sucked” in ahead of the front proper. We conclude that the irregularities are caused by the strongly varying local capillary pressure functions. One could call these irregularities therefore “capillary fingering” [see e.g. 31].

Varying the water viscosity, we have also reviewed cases close to the switch-over point from stable to unstable displacement as predicted by the new criterion (around $\mu_w = 0.27\text{cP}$ for our data set). The saturation maps were not really different just below or just over the switch point. We interpret this as the initial growth rate of the fingers being too small to become visible on the time scale of the experiments. The initial growth rate will be proportional to $(\partial q/\partial t)_{\Delta P}$, which is just above zero when above, but close to, the switching point.

Finally, we have revisited the stability screening work as was published by Berg and Ott [29]. We focused on their “Case a” that was deemed stable at the time. We calculate for that case $M_{s_hag} = 1.0$ and $M_\alpha = 0.7$, so unstable according to the new criterion. First, we duplicated their results, using a flat permeability distribution with a width of $\pm 2\text{mD}$ around a mean of 100mD and homogeneous $P_c(S_w)$ as specified in [29]. We observed no fingering in the saturation map, in line with what was reported in [29]. Subsequently, we simulated *Case a* using the same approach as discussed above: we implemented a Gaussian porosity distribution with standard deviation of 0.02 and a log-normal permeability distribution. The local capillary pressure function in each grid block was made dependent on

the local porosity and permeability as discussed above. This time, the saturation map shows clear fingering (Fig. 4).

This demonstrates the impact of the triggering mechanism in simulations to study fingering: a flat permeability distribution together with a homogeneous $P_c(S_w)$ apparently was less successful in promoting fingering than our present approach.



Fig. 4. “Case a” of Berg and Ott [29] revisited, Gaussian porosity and log-normal permeability distribution applied, all other parameters set to values published in [29]. Fingering is observed, in line with the new criterion.

One may argue that one approach is more realistic than another, but in fact the choice remains very subjective. For instance, we may as well have chosen a standard deviation of 0.01 or 0.04 rather than 0.02 for the Gaussian porosity distribution. Detailed measurements of the actual porosity and permeability distributions of the rock would be required to resolve this.

We have also used the new criterion to re-evaluate the stability map shown in Fig. 4 of Berg and Ott [29]. The picture has changed significantly. Displacement is unstable for nearly all points in that figure, except for some points in the top right-hand corner. Stability is calculated for n_{CO_2} between 4.0 and 5.0, if n_{brine} equals 4.5 or 5.0; and for the single point with $n_{CO_2} = 4.0$, $n_{brine} = 5.0$. The contour lines as shown in Fig. 4 of Berg and Ott [29] do not exist anymore: one needs to set-up contour lines for M_{s_hag} in one plot and for M_α in another and then select the points for which holds $M_{s_hag} < M_\alpha$.

Another issue that has come to light now is that also the identification of fingering with a saturation map is highly subjective. Just comparing the fingering in Fig. 4 with the “fingering” in Fig. 3 illustrates this. It is physically impossible that the parameter choice used for Fig. 3 would generate viscous fingers (viscosity of the injected phase is twice as large as that of the displaced phase), but clearly the front is not flat because of the capillary heterogeneity. Fig. 18 in of Berg and Ott [29] provides another reason why saturation maps may not be a reliable way of determining fingering because they are the consequence of numerical simulations with a specific choice of scale, but for $P_c \neq 0$ the visco-capillary balance causes the fingers to appear potentially at a larger scale than simulated.

All-in-all we conclude that saturation maps are not a good tool to establish objectively whether fingering occurs.

4 Impact of fingering on SCAL measurements

The impact of fingering on production behaviour has been studied by various authors, both on the scale of the field [e.g. 52, 53, and 54] and on the scale of the core plug in the

laboratory [e.g. 55, 56, and 57]. A general problem, both in the field as well as in the laboratory is that heterogeneity may have a strong and often unknown impact that may enhance the effect of fingering.

As discussed above, the base of our simulation study is a well-defined characterisation of the permeability variability through the parameter V . As shown in [46], the chosen value of $V = 0.42$ gives rise to porosity and permeability distributions that will not affect the relative permeabilities determined in a SCAL experiment, when state-of-the-art history matching is applied of the production data obtained from stable displacements. We have now extended the work to unstable displacements.

Our approach was to compare the relative permeabilities characterisations generated by the automatic history matching tool AutoSCORES [46] on a stable drive with the results obtained on an unstable drive. To that end, we took the production data of the synthetic drainage experiments discussed in section 3.1, for the case with $\mu_w = 0.01\text{cP}$ (so stable by all criteria) and for the case with $\mu_w = 10\text{cP}$ (so unstable by all criteria). We ran AutoSCORES to extract the Corey description for the relative permeabilities and compared that with the “truth”, i.e. the input data for the relative permeability and capillary pressure data used in the 2-D simulations. Since AutoSCORES is based on the Levenberg-Marquardt method, also estimates on the standard deviation of each parameter are reported [46, 58]. It appeared that the difference between the two sets of Corey parameters was statistically insignificant, and that the difference of each with the “truth” data also was statistically insignificant, in both cases at the 5% as well as at the 1% level of significance. However, running AutoSCORES to history match flooding experiments in isolation is risky: the reported standard deviations generally are large even when matches themselves may appear to look “well”. This has an immediate impact on the outcome of the statistical analysis. At this stage, one would need to run a synthetic multi-speed centrifuge experiment and set-up an analysis of the synthetic USS and centrifuge data combined. In view of the already large run times for the USS simulations, we decided not to go that route. Instead, we chose to investigate the situation through laboratory experiments.

5 Experimental program

To test our conclusions in section 4, we have conducted an experimental program consisting of unsteady-state experiments in drainage mode at two extreme viscosity ratios. As explained and demonstrated in [46], it is possible to assess the significance of seemingly different experimental outcomes, even using a small set of three or so experiments, by applying the appropriate statistics frame work. With this in mind, we ran one experiment at a very unfavourable viscosity ratio to compare with a set of three experiments at a favourable viscosity ratio.

5.1 Experimental design

As before [46], we used Obernkirchener (OBKN) sandstone outcrop samples and the simulator SCORES [45] for the detailed design. The drainage experiments were augmented

with one bump (increased flow rate) flood. The base case runs were conducted on samples B2 (twice) and G2, with a Klinkenberg corrected permeability of about 5 mD and 10 mD respectively. As injection fluid we used a mineral oil with a viscosity of about 3 cP, to displace brine with a viscosity of about 1 cP. The samples are saturated initially at 100% brine. The initial injection rate was at 0.2 cm³/min, bumped to 1 cm³/min after some 4 hours.

For the experiment at unfavourable viscosity ratio we used Isopar L with a viscosity of 1.4 cP to displace a glycerol-water mixture with a viscosity of 87 cP. Also in this experiment, the sample initially is saturated at 100% glycerol mixture. Initial flow rate was set at 0.2 cm³/min, bumped to 2 cm³/min after about 19 hrs.

At the end of each experiment Dean-Stark was executed to verify material balance. For the glycerol experiment we checked material balance through NMR.

In the design phase, estimating $k_{r\text{wor}}$ at 0.5, we calculated M_{end} at 0.67 for the mineral oil displacing brine, possibly not quite a safe value for stable displacement with the new criterion requiring $M_{\text{end}} < \alpha$ (section 2.7), and generally $0.3 < \alpha < 0.7$. However, with P_c estimated for OBKN as before [46], SCORES simulations showed $d\Delta P(t)/dt > 0$ before breakthrough, indicative of stable displacement (section 3.1). This was subsequently borne out in each of the three base case experiments.

For the glycerol experiment, we estimated M_{end} at 130 and $M_{s_{\text{hag}}}$ at 1.4. These numbers are clearly indicating unstable displacement, which was also borne out both by the SCORES design run and by the experiment: we observed $d\Delta P(t)/dt < 0$ before breakthrough.

At the end of the experiments, AutoSCORES was used to interpret the production data in terms of the Corey parameters for the relative permeabilities, just as we did for the synthetic cases in section 4. To constrain the solutions, we fed AutoSCORES the data of the multi-speed centrifuge experiment that measured P_c , similar to our approach in [46]. The results are listed in Table 1.

Table 1. Corey parameters from AutoSCORES, determined through history matching the three base case experiments and one experiment with glycerol, each combined with the data of a multi-speed centrifuge experiment.

| Exp/Param | S_{wc} | $k_{r\text{wor}}$ | n_w | n_o |
|-------------|-----------------|-------------------|-----------|-----------|
| B1.1 base | 0.06±0.03 | 0.61±0.11 | 4.16±0.16 | 3.18±0.20 |
| G2 base | 0.04±0.02 | 0.47±0.02 | 4.35±0.23 | 2.11±0.16 |
| B1.2 base | 0.04±0.01 | 0.56±0.05 | 4.80±0.18 | 2.72±0.17 |
| G2 glycerol | 0.01±0.01 | 0.23±0.01 | 4.87±0.21 | 2.95±0.08 |

The two missing Corey parameters S_{or} and $k_{r\text{orc}}$ were kept constant at 0.01 and 0.98 respectively. Note that in these drainage experiments S_{or} should be taken as the percolation threshold saturation. The outcome of the history matching is not sensitive to its exact small value, for which we just used an estimate based on experience. The standard deviations reported in Table 1 are estimated by AutoSCORES, as discussed in [46].

5.2 Statistical analysis of the AutoSCORES results

At first glance, it may appear that the data in Table 1 show quite some overlap, given the reported standard deviations, and that therefore the Corey parameters of the unstable glycerol experiment, or at least most of these, cannot be distinguished from the Corey parameters of the base case stable experiments.

Similar to our earlier work, a statistical analysis was conducted by testing for the formal “H₀” hypothesis that says: “there is no significant difference between the Corey parameters of the base case experiments and of the glycerol experiment”, using a t-test [46]. As mentioned in [46], a t-test considers the difference between two averages, using the respective standard deviations and the number of simulations in the SCAL experiments. The calculated t-value is then compared against a critical test value at a 5% (or 95% confidence) or 1% (or 99% confidence) test level found from a standard table of the t-probability density distribution [59]. For the data in Table 1 we found that the hypothesis is to be rejected on both levels of statistical significance. In other words: the -unstable- glycerol experiment shows Corey parameters that do deviate from the -stable- base case.

It is important to note that this conclusion could only be reached after interpreting the USS data with the centrifuge data combined with AutoSCORES. The results from an history match of USS “solo” are just not reliable enough for such assessment.

6 Conclusions

- We have presented a new concept to build a criterion for the onset of instability in 2-phase displacement. The new criterion encompasses all historic criteria for the onset of instability: these are special cases of our more general formulation.
- Also the Dietz criterion [7] for macroscopic displacement stability in the field is shown to be a special case of the new more general formulation.
- Displacement will be stable if $M_{end} \leq \alpha < 1$, with $0 < \alpha < 1$, different from the common assumption of stability for $M_{end} < 1$.
- For $M_{end} > \alpha$, the new criterion is more restrictive than Hagoort’s [21] criterion, because we have now $M_{s_hag} < M_{\alpha} < 1$ as a requirement for stable displacement, if gravity is assumed zero.
- For $M_{end} > \alpha$ and non-zero gravity, there exists a critical flow rate for stability that is shown to be related to Hagoort’s “free fall filter velocity” [44]. As a result, Dietz’s critical rate needs to be modified.
- Saturation maps are not a good tool for an objective assessment whether fingering occurred.
- The new criterion provides a necessary but not a sufficient condition for the onset of fingering. Fingering may not develop due to capillary forces, or due to the effect of gravity, or due to spatial or other boundary conditions, or due to e.g. perfect homogeneity of the rock (i.e. $V = 0$).
- It is important to present results in the context of statistical significance.

- It is recommended to conduct history matching of flooding experiments and multi-speed centrifuge experiments combined to constrain the results and improve the statistical significance.
- Laboratory experiments were successfully used to demonstrate the impact of fingering onto SCAL measurements in unsteady-state experiments.
- A quantitative assessment of heterogeneity is an important part of the study into the impact of fingering, both for SCAL as well as for the field.

Nomenclature

| | | |
|--------------------|----------------------|--|
| f | [-] | fractional flow |
| G | [m.Pa.s] | defined in Eq. A5 |
| g | [m/s ²] | gravity constant |
| H | [kg/m ²] | defined in Eq. A6 |
| K | [m ²] | permeability |
| k _r | [-] | relative permeability |
| L | [m] | distance between injection and production |
| M _{end} | [-] | mobility ratio at end-point saturations (defined in Eq. A19) |
| M _{sh} | [-] | mobility ratio at shock front (defined in Eq. A29) |
| M _{s_hag} | [-] | Hagoort shock front mobility ratio (defined in Eq. A18) |
| M _α | [-] | limit used in new criterion for onset instability (defined in Eq. A21) |
| M _μ | [-] | viscosity ratio, equal to μ ₂ /μ ₁ |
| n | [-] | Corey exponent, as defined in [46] |
| P | [Pa] | pressure |
| q | [m/s] | flow rate m/s |
| R | [Pa.s] | defined in Eq. A2a |
| R _p | [kg/m ³] | defined in Eq. A2b |
| S | [-] | saturation |
| t | [s] | time |
| V | [-] | homogeneity number (defined in [50]) |
| v | [m/s] | velocity |
| x | [m] | distance |

Greek

| | | |
|---|----------------------|---------------------|
| α | [-] | given in Eq. A16 |
| β | [-] | given in Eq. A26 |
| Δ | | difference operator |
| θ | [degrees] | angle |
| φ | [-] | porosity |
| μ | [Pa.s] | viscosity |
| ρ | [kg/m ³] | density |

subscripts

| | |
|----|-----------------|
| I | invading phase |
| 2 | displaced phase |
| c | capillary |
| fr | shock front |
| s | solvent |
| o | oil |
| or | residual oil |
| w | water |
| wc | connate water |

superscripts

‘ first derivative

The CT-scans of the OBKN material were made available courtesy of Prof. Pacelli Zitha, TUDelft, and conducted expertly by Mrs. Ellen Meijvogel-de Koning. The glycerol/oil interfacial tension was measured by DataPhysics Instruments GmbH, using an OCA25 pendant drop system. We thank Dario Santonico for his energetic and professional managing and overall support of the flow experiments.

References

1. W.S. Jevons, On the cirrus form of cloud, *Phil. Mag. J. Sc.* 4th Series, **14**, 90, 22-35 (1857)
2. Lord Rayleigh, Investigation of the character of equilibrium of an incompressible heavy fluid of variable density, *Proc. Lond. Math. Soc.* **14**, 170–177 (1883)
3. J.W. de Korver and H.L. Douwes Dekker, Enkele beschouwingen over het aardolieveld Schoonebeek, 1948-1949 Jaarboek der Mijnbouwkundige Vereeniging te Delft, Delft. Uitg. Mij. Delft (1949)
4. G. Taylor, The instability of liquid surfaces when accelerated in a direction perpendicular to their planes. I, *Proc. R. Soc. Lond. A* **201**, 192–196 (1949)
5. D.J. Lewis, The instability of liquid surfaces when accelerated in a direction perpendicular to their planes. II, *Proc. R. Soc. Lond. A* **202**, 81–96 (1949)
6. S. Hill, Channeling in packed columns, *Chem. Eng. Sc.* **1** (6) 247-253 (1952)
7. D. Dietz, A theoretical approach to the problem of encroaching and by-passing edge water, *Proc. Kon. Ned. Akad. Wetenschap.* **B56**, 83-92 (1953)
8. L.P. Dake, *Fundamentals of reservoir engineering*, Elsevier 1978
9. F.J. Fayers and A. Muggeridge, Extensions to Dietz theory and behavior of gravity tongues in slightly tilted reservoirs, SPE-18438 (1990)
10. P.G. Saffman and G. Taylor, The penetration of a fluid into a porous medium or Hele-Shaw cell containing a more viscous liquid, *Proc. R. Soc. Lond. A* **245**, 312–329 (1958)
11. H.S. Hele-Shaw, Experiments on the nature of the surface resistance in pipes and on ships, *Trans. Inst. Naval Archit.* **39**, 145-156 (1897)
12. D. Bensimon, Stability of viscous fingering, *Phys. Rev. A* **33**, 1302-1308 (1986)
13. M. Mineev-Weinstein, Selection of the Saffman Taylor finger width in the absence of surface tension: an exact result, *Phys. Rev. Lett.* **80** (10), 2113-2116 (1998)
14. S. Tanveer, Surprises in viscous fingering, *J. Fluid Mech.* **409**, 273-308 (2000)
15. G.M. Homsy, Viscous fingering in porous media, *Ann. Rev. Fluid Mech.* **19**, 271-311 (1987)
16. R.L. Chuoke, P. van Meurs, and C. van der Poel, The instability of slow, immiscible, viscous liquid-liquid displacements in permeable media, SPE-1141-G (1959)
17. E.D. Chikhliwala, A.B. Huang, and Y.C. Yortsos, Numerical study of the linear stability of immiscible displacement in porous media, *Transp. Porous Med.* **3**, 257-276 (1987)
18. A. Riaz and E. Meiburg, Three-dimensional miscible displacement simulations in homogeneous porous media with gravity override, *J. Fluid Mech.* **494**, 95-117 (2003)
19. A.E. Kampitsis, W.J. Kostorz, A.H. Muggeridge, and M.D. Jackson, The life span and dynamics of immiscible viscous fingering in rectilinear displacements, *Phys. Fluids* **33**, 096608 (2021); doi: 10.1063/5.0064955
20. J.M. Dumoré, Stability considerations in downward miscible displacements, SPE-961-PA (1964)
21. J. Hagoort, Displacement stability of water drives in water-wet connate-water-bearing reservoirs, SPE-4268-PA (1974)
22. E.J. Peters and D.L. Flock, The onset of instability during two-phase immiscible displacement in porous media, SPE-8371 (1979)
23. J.W. Sheldon, On the fingering of slow, immiscible, viscous liquid-liquid displacements, SPE-1552-G (1960)
24. S. Bachu and G. Dagan, Stability of displacement of a cold fluid by a hot fluid in a porous medium, *Phys. Fluids* **22** (1), 54-59 (1979)
25. J.W. McLean, I The fingering problem in flow through porous media; II The kinetic equation for hamiltonian systems, Thesis, Cal. Inst. Techn. (1980)
26. A.B. Huang, E.D. Chikhliwala, and Y.C. Yortsos, Linear stability analysis of immiscible displacement including continuously changing mobility and capillary effects: Part II - General basic flow profiles, SPE-13163-MS (1984)
27. J.N.M. van Wunnik and K. Wit, A simple analytical model of the growth of viscous fingers in heterogeneous porous media, Conf. Proc. 1st ECMOR, Cambridge UK, July 1989
28. A.P. Aldushin and B.J. Matkowsky, Selection in the Saffman Taylor finger problem and the Taylor Saffman bubble problem without surface tension, *Appl. Math. Lett.* **11** (6) pp 57-62 (1998)
29. S. Berg and H. Ott, Stability of CO₂-brine immiscible displacement, *Int. J. Greenhouse Gas Control* **11**, 188-203 (2012)
30. G. Coskuner and R.G. Bentsen, A new approach to the onset of instability for miscible fluid - fluid displacements in porous media, SPE-16475 (1987)
31. R. Lenormand, E. Touboul, and C. Zarcone, Numerical Models and Experiments on Immiscible Displacements in Porous Media, *J. Fluid Mech.* **189**, 165-187 (1988)
32. E. Lajeunesse, J. Matin, N. Rakotomalala, D. Salin, and Y.C. Yortsos, Miscible displacement in a Hele-Shaw cell at high rates, *J. Fluid Mech.* **398**, 299-319 (1999)

33. F.F. Craig Jr, T.M. Geffen, and R.A. Morse, Oil recovery performance of pattern gas and water injection operations from model tests, SPE-413-G (1954)
34. A. Skauge, K. Sorbie, P.A. Ormehaug, and T. Skauge, Experimental and numerical modeling studies of viscous unstable displacement, 15th Eur. Symp. Impr. Oil Rec., Paris, France, April 27-29, paper A28 (2009)
35. J. Peters and S. Khataniar, The effect of instability on relative permeability curves obtained by the dynamic-displacement method, SPE-14713-PA (1987)
36. H.K. Sarma and R.G. Bentsen, An experimental verification of a modified instability theory for immiscible displacements in porous media, J. Can. Petr. Tech. **26** (4), 88-99 (1987)
37. G.-Q. Tang and A.R. Kovscek, High resolution imaging of unstable, forced imbibition in Berea sandstone, Transp. Porous Med. **86** 617-634 (2011)
38. H. Ott, S. Berg and S. Oedai, Displacement and mass transfer of CO₂-brine in sandstone, En. Proc. **23**, 512-520 (2012)
39. S. Bouquet, S. Leray, F. Douarche, and F. Roggero, Characterisation of viscous unstable flow in porous media at pilot scale - Application to heavy oil polymer flooding, IOR 2017-19th Eur. Symp. Impr. Oil Rec. 1, 1-30 (2017)
40. S.E. Buckley and M.C. Leverett, Mechanism of fluid displacement in sands, Trans. AIME **146**, 107-116 (1942)
41. R.A. Wooding, The stability of a viscous liquid in a vertical tube containing porous material, Proc. R. Soc. Lond. A **252** 120–134 (1959)
42. R. Lenormand, K. Lorentzen, J.G. Maas, and D. Ruth, Comparison of four numerical simulators for SCAL experiments, SCA2016-006 (2016)
43. S. Berg, H. van der Linde, N. Brussee, M. Rücker, H. Dijk, E. Unsal, T.G. Sorop, and M. Appel, Physical origin of pressure- and saturation fluctuations in steady-state core floods, SCA2021-020 (2021)
44. J. Hagoort, Oil recovery by gravity drainage, SPE- 7424 (1980)
45. J.G. Maas, B. Flemisch, and A. Hebing, “Open source simulator DuMux available for SCAL data interpretation”, SCA2011-08 (2011)
46. J.G. Maas, N. Springer, and A. Hebing, Defining a sample heterogeneity cut-off value to obtain representative Special Core Analysis (SCAL) measurements, SCA2019-024 (2019)
47. D.W. Peaceman and H.H. Rachford Jr., Numerical calculation of multidimensional miscible displacement, SPE-1524-G (1960)
48. P. Sigmund, H. Sharma, D. Sheldon, and K. Aziz, SPE-14368 (1988)
49. A. Riaz and E. Meiburg, Vorticity interaction mechanisms in variable-viscosity heterogeneous miscible displacements with and without density contrast, J. Fluid Mech. **517**, 1-25, 2004
50. J.G. Maas and A. Hebing, “Quantitative X-ray CT for SCAL plug homogeneity assessment”, SCA2013- 004 (2013)
51. H. Dykstra and R.L. Parsons, The prediction of oil recovery by water flood, Secondary recovery of oil in the United States, 2nd edition, API, 160-174 (1950)
52. E.J. Koval, A method for predicting the performance of unstable miscible displacement in heterogeneous media, SPE-450 (1963)
53. M.R.Todd and W.J. Longstaff, The development, testing, and application of a numerical simulator for predicting miscible flood performance, SPE-3484 (1972)
54. F.J. Fayers, M.J. Blunt, and M.A. Christie, Comparisons of empirical viscous-fingering models and their calibration for heterogeneous problems, SPE-22184 (1992)
55. H.S. Al-Shuraiqi, C.A. Grattoni, and A.H. Muggeridge, Numerical and experimental investigation into the effects of viscosity and injection rate on relative permeability and oil recovery, SCA2005-40 (2005)
56. H. Luo, K.K. Mohanty, M. Delshad, and G.A. Pope, Modeling and upscaling unstable water and polymer floods: dynamic characterization of the effective finger zone, SPE-179648-MS (2016)
57. B.M. Ferreira Pereira, Accounting for viscous fingering in relative permeability estimation of special core analysis measurements, Thesis, Herriot-Watt (2017)
58. S. Berg, E. Unsal, and H. Dijk, Non-uniqueness and uncertainty quantification of relative permeability measurements by inverse modelling, Comp. Geotech. **132** (2021) 103964 (2021)
59. R.A. Fisher, F. Yates, “Statistical tables for biological, agricultural and medical research”, London, Oliver & Boyd (1963)

Appendix A. Derivation of a general criterion for the onset of instability

The onset of instability occurs at $(\partial q/\partial t)_{\Delta P} > 0$ (see main text), so we analyse $(\partial q/\partial t)_{\Delta P}$. Consider liquid 1 to be injected, to displace liquid 2. Define $q = q_1 + q_2$, assume incompressible flow, assume $P_c=0$, use angle θ with respect to the horizontal, apply Darcy’s equation to each phase and add, we find for 1-D flow [8]

$$q = -K \left\{ \left[\frac{k_{r1}(S)}{\mu_1} + \frac{k_{r2}(S)}{\mu_2} \right] \frac{dp}{dx} + g \sin(\theta) \left[\rho_1 \frac{k_{r1}(S)}{\mu_1} + \rho_2 \frac{k_{r2}(S)}{\mu_2} \right] \right\} \quad (A1)$$

Noting that $S = S(x, t)$ and in order to simplify the notation, define

$$R = R(x, t) = \left[\frac{k_{r1}(S)}{\mu_1} + \frac{k_{r2}(S)}{\mu_2} \right]^{-1} \quad (A2a)$$

and

$$R_\rho = R_\rho(x, t) = \frac{[\rho_1 \frac{k_{r1}(S)}{\mu_1} + \rho_2 \frac{k_{r2}(S)}{\mu_2}]}{[\frac{k_{r1}(S)}{\mu_1} + \frac{k_{r2}(S)}{\mu_2}]} \quad (\text{A2b})$$

and define pressure drop ΔP from inlet to outlet

$$\Delta P = - \int_{p(x=0)}^{p(x=L)} dp \quad (\text{A3})$$

we get

$$\Delta P = \frac{q}{K} \int_0^L R dx + g \sin(\theta) \int_0^L R_\rho dx \quad (\text{A4})$$

Define

$$G = G(t) = \int_0^L R dx \quad (\text{A5})$$

and

$$H = H(t) = \int_0^L R_\rho dx \quad (\text{A6})$$

Combining Eqs. A4, A5 and A6, gives

$$\Delta P(t) = K^{-1} q(t) G(t) + g \sin(\theta) H(t) \quad (\text{A7})$$

Take the total derivative with respect to t at constant pressure drop and solve for $(\partial q / \partial t)_{\Delta P}$:

$$\left(\frac{\partial q}{\partial t} \right)_{\Delta P} = - \frac{q}{G} \left(\frac{\partial G}{\partial t} \right)_{\Delta P} - K \frac{g \sin(\theta)}{G} \left(\frac{\partial H}{\partial t} \right)_{\Delta P} \quad (\text{A8})$$

As mentioned before, a drive will experience the onset for instability if $\frac{\partial q}{\partial t} > 0$. So with q and G positive, the onset occurs for

$$\frac{\partial G}{\partial t} < \frac{-K g \sin(\theta) \partial H}{q \partial t} \quad (\text{A9})$$

Note that for a horizontal 1D case ($\theta = 0$), condition A9 simplifies into

$$\frac{\partial G}{\partial t} < 0 \quad (\text{A10})$$

as condition for the onset of instability while the flow rate q does not play a role for the onset.

A.1 Calculation and interpretation of $\partial G / \partial t$

Consider a drive, liquid 1 displacing liquid 2 in 1-D, with $S_1 = S_{1r}$ downstream of the displacement front. Breaking up the integral in Eq. A8 into two parts; before and after the shock front $x_{fr}(t)$ we obtain

$$G(t) = \int_0^{x_{fr}(t)} R dx + (L - x_{fr}(t)) \left[\frac{k_{r2_end}}{\mu_2} \right]^{-1} \quad (\text{A11})$$

Take first derivative (employing chain rule including boundary of integral):

$$\frac{\partial G}{\partial t} = R(S_{fr}) \frac{\partial x_{fr}}{\partial t} + \int_0^{x_{fr}(t)} \left(\frac{\partial R}{\partial t} \right)_x dx - \frac{\partial x_{fr}}{\partial t} \left[\frac{k_{r2_end}}{\mu_2} \right]^{-1} \quad (\text{A12})$$

We have

$$\int_0^{x_{fr}(t)} \left(\frac{\partial R}{\partial t} \right)_x dx = \int_{R(1-S_{2r})}^{R(S_{fr})} - \left(\frac{\partial x}{\partial t} \right)_{S(R)} dR \quad (\text{A13})$$

Applying the mean value theorem, we obtain

$$\int_{R(1-S_{2r})}^{R(S_{fr})} - \left(\frac{\partial x}{\partial t} \right)_{S(R)} dR = - \left(\frac{\partial x}{\partial t} \right)_{S_{1m}} \{ R(S_{fr}) - R(1 - S_{2r}) \} = - \left(\frac{\partial x}{\partial t} \right)_{S_{1m}} \left\{ R(S_{fr}) - \left[\frac{k_{r1_end}}{\mu_1} \right]^{-1} \right\} \quad (\text{A14})$$

with value for S_{1m} unknown at this point with $S_{fr} < S_{1m} < 1 - S_{2r}$. Transforming the velocity at S_{1m} into a scaling factor in relation to shock front velocity

$$\left(\frac{\partial x}{\partial t} \right)_{S_{1m}} = \alpha \left(\frac{\partial x}{\partial t} \right)_{S_{fr}} \quad (\text{A15})$$

i.e. transforming S_{1m} into α , with $0 < \alpha < 1$. It can be proven that

$$\alpha = \frac{\int_{(1-S_{2r})}^{S_{fr}} f_1'(S) R'(S) dS}{f_1'(S_{fr}) \left\{ R(S_{fr}) - \left[\frac{k_{r1_end}}{\mu_1} \right]^{-1} \right\}} \quad (\text{A16})$$

Note this expression is amenable to numerical integration to calculate α .

Combining Eqs. A12, A13, A14, and A15 we have

$$\frac{\partial G}{\partial t} = \left(\frac{\partial x}{\partial t} \right)_{S_{fr}} \left\{ R(S_{fr})(1 - \alpha) + \alpha \left[\frac{k_{r1_end}}{\mu_1} \right]^{-1} - \left[\frac{k_{r2_end}}{\mu_2} \right]^{-1} \right\} \quad (\text{A17})$$

Note from the definition of the Hagoort shock-front ratio [21] and Eq. A2, we have

$$M_{s_hag} = \frac{k_{r1}(S_{fr})/\mu_1 + k_{r2}(S_{fr})/\mu_2}{k_{r2_end}/\mu_2} = R^{-1}(S_{fr}) \left[\frac{k_{r2_end}}{\mu_2} \right]^{-1} \quad (\text{A18})$$

Define the end-point mobility ratio as the ratio of the saturation end-point mobility of the injected liquid 1 over the saturation end-point mobility of the displaced liquid 2:

$$M_{end} = \frac{\frac{k_{r1_end}}{\mu_1}}{\frac{k_{r2_end}}{\mu_2}} \quad (\text{A19})$$

For $\theta = 0$ (so in the absence of gravity), apply Eq. A17 to condition A10, and using $\partial x_{fr} / \partial t > 0$, we find as stability criterion for the onset of instability

$$\left[\frac{k_{r2_end}}{\mu_2} \right]^{-1} (1 - \alpha) \left\{ \frac{1}{M_{s_hag}} - \frac{(1 - \frac{\alpha}{M_{end}})}{(1 - \alpha)} \right\} < 0 \quad (\text{A20})$$

For $M_{end} = \alpha$, we have stable displacement because condition A20 cannot be fulfilled, irrespective of the value of M_{s_hag} , since we have $0 < \alpha < 1$ (and $M_{s_hag} > 0$).

For $M_{end} \neq \alpha$, we can define

$$M_\alpha = \frac{1 - \alpha}{1 - \frac{\alpha}{M_{end}}} \quad (\text{A21})$$

Combining Eqs. A21 and A20, we find as criterion for the onset of instability

$$\left\{ \frac{1}{M_{s_hag}} - \frac{1}{M_\alpha} \right\} < 0 \quad (A22)$$

We have two cases

$M_{end} < \alpha$: therefore $M_\alpha < 0$ (see Eq. A21), so condition A22 is never fulfilled, i.e. displacement will be stable for any value of M_{s_hag} .

$M_{end} > \alpha$: From the condition A22, we find for the onset of instability for $M_{s_hag} > M_\alpha$, or vice versa stable displacement for

$$M_{s_hag} < M_\alpha < 1 \quad (A23)$$

Note that this condition is more restrictive than the original Hagoort criterion that predicts stability for $M_{s_hag} < 1$.

A.1 Calculation and interpretation of $\partial H/\partial t$

Consider a drive liquid 1 displacing liquid 2 in 1-D, with $S_1=S_{1r}$ downstream of the displacement front. Similar to Eq. A11 we have

$$H(t) = \int_0^{x_{fr}(t)} R_\rho dx + (L - x_{fr}(t))\rho_o \quad (A24)$$

Analogous to Eq. A17 we find for the first derivative

$$\frac{\partial H}{\partial t} = \left(\frac{\partial x}{\partial t} \right)_{S_{fr}} \{ R_\rho(S_{fr})(1 - \beta) + \beta\rho_1 - \rho_2 \} \quad (A25)$$

with β defined analogous to α (see Eqs. A14 and A15) and can be numerically calculated (analogous to Eq. A16) through

$$\beta = \frac{\int_{(1-S_{2r})}^{S_{fr}} f_1'(s) R_\rho'(s) ds}{f_1'(S_{fr}) \{ R_\rho(S_{fr}) - \rho_1 \}} \quad (A26)$$

Combining Eqs. A9, A17 and 25 into an expression for the criterion for the onset of instability gives

$$\left\{ R(S_{fr})(1 - \alpha) + \alpha \left[\frac{k_{r1_end}}{\mu_1} \right]^{-1} - \left[\frac{k_{r2_end}}{\mu_2} \right]^{-1} \right\} < \frac{-Kgsin(\theta)}{q} \{ R_\rho(S_{fr})(1 - \beta) + \beta\rho_1 - \rho_2 \} \quad (A27)$$

Use definition of M_{s_hag} (Eq. A18) and of M_{end} (Eq. A19) we have for the onset of instability

$$\left\{ \frac{(1-\alpha)}{M_{s_hag}} + \frac{\alpha}{M_{end}} - 1 \right\} < \frac{-Kgsin(\theta)}{q} \left[\frac{k_{r2_end}}{\mu_2} \right] \{ R_\rho(S_{fr})(1 - \beta) + \beta\rho_1 - \rho_2 \} \quad (A28)$$

We have two cases:

1) $M_{end} \neq \alpha$

Define mobility ratio at the front M_{sh} , analogous to the end point mobility ratio M_{end}

$$M_{sh} = \left(\frac{k_{r1}}{\mu_2} \right)_{S=S_{fr}} \quad (A29)$$

and define

$$\Delta\rho = \rho_1 - \rho_2 \quad (A30)$$

Define characteristic drainage rate q_{char} (see Hagoort's "free fall filter velocity" in [44])

$$q_{char} = K\Delta\rho gsin(\theta) \left[\frac{k_{r2_end}}{\mu_2} \right] \quad (A31)$$

Using the definition of M_α (Eq. A21), R_ρ (Eq. A2b), M_{sh} , $\Delta\rho$, and q_{char} , the condition for the onset of instability A28 is rewritten as

$$\left\{ \frac{1}{M_{s_hag}} - \frac{1}{M_\alpha} \right\} < \frac{-q_{char} (M_{sh} + \beta)}{q(1-\alpha) (M_{sh} + 1)} \quad (A32)$$

With $0 < \alpha < 1$, $0 < \beta < 1$ and $0 < \theta < \pi/2$, we have that the right hand side of condition A32 is always negative.

We have two situations, Case 1 and Case 2 as follows:

Case 1a: $M_{end} < \alpha$

In this case $M_\alpha < 0$, so A32 is never fulfilled and we have stable displacement for any value of M_{s_hag} and at any flow rate.

Case 1b: $M_{end} > \alpha$

In this case we have $0 < M_\alpha < 1$.

For $M_{s_hag} \leq M_\alpha$, we have no onset for stability irrespective whether gravity is active because condition A32 is never fulfilled.

In the event that $M_{s_hag} > M_\alpha$ we have stability for

$$q \leq \frac{q_{char} (M_{sh} + \beta)}{(1-\alpha) (M_{sh} + 1)} \left[\frac{1}{M_\alpha} - \frac{1}{M_{s_hag}} \right]^{-1} \quad (A33)$$

Summarising: relation A33 imposes a critical rate for stability in the presence of gravity, but only for $M_{s_hag} > M_\alpha$. So, despite $M_{s_hag} \leq M_\alpha$ would not be honoured, gravity brings about a stabilising effect, up to a critical rate (as in the classical stability criteria for viscous fingering derived by linear stability analysis). Above this rate, viscous forces counter balance gravity and the onset of fingering is surpassed. There is no rate dependency for the onset of fingering if $M_{s_hag} \leq M_\alpha$.

Case 2: $M_{end} = \alpha$

From the form of A32, we see that the right hand side of condition A28 is always negative, so for $M_{end} = \alpha$ we have condition A28 is never fulfilled, i.e. we have always stable displacement irrespective of flow rate, and for any value of M_{s_hag} .